Computation of low-frequency loads by the middle-field formulation

Yi-Shan Dai‡, Xiao-Bo Chen†, & Wen-Yang Duan‡

†Research Department, Bureau Veritas, 17bis, Place des Reflets, 92400 Courbevoie (France)
Fax: +33-1-4291.3395 Email: xiao-bo.chen@bureauveritas.com

‡College of Shipbuilding Engineering, Harbin Engineering University, 150001 Harbin (China)

The low-frequency wave load is well known to be the main source of excitation to offshore or near shore moored FPSO systems. The accuracy of its evaluation is critically important in the time simulation of large slow-drift motions since the results of motion simulations determine the design of mooring systems. The near-field formulation derived from the pressure integration is largely used and considered to be the only way to go, unlike the constant drift load for which the far-field formulation based on the momentum theorem is available as well. However, the near-field formulation is reputed by its poor precision and convergence, especially for structure's hull with sharp geometrical variations. Very recently, the new formulations for the second-order wave load are developed in Chen (2004). In particular, the middle-field formulation derived from the near-field formulation by using the variants of Stokes' theorem given in Dai (1998) and Green's theorem gives results of drift loads much better, as accurate as the far-field formulation. The application of the middle-field formulation to compute the low-frequency wave loads is presented here.

QTF of low-frequency wave loads

The second-order low-frequency wave load takes place at the frequency equal to the difference of wave frequencies. In bichromatic waves, the first-order quantities are written as :

$$(\Phi,\mathcal{E},\mathbf{X},\mathbf{T},\mathbf{R}) = \Re\{a_0^j(\phi^j,\eta^j,\mathbf{x}^j,\mathbf{T}^j,\mathbf{R}^j)e^{-i\omega_j t} + a_0^k(\phi^k,\eta^k,\mathbf{x}^k,\mathbf{T}^k,\mathbf{R}^k)e^{-i\omega_k t}\} \tag{1}$$

where $(\phi,\mathcal{E},\mathbf{X},\mathbf{T},\mathbf{R})$ stand for the velocity potential, free-surface elevation, body's displacement, translation and rotation vectors. In (1), (a_0^j,a_0^k) stand for the amplitudes of incoming waves at frequencies (ω_j,ω_k), respectively. The loads can be decomposed into a part depending only on the first-order quantities and another on the second-order potential :

$$(\mathbf{F}^-,\mathbf{M}^-) = \Re\left\{a_0^j\overline{a}_0^k(\mathbf{f}^-,\mathbf{m}^-)e^{-i(\omega_j-\omega_k)t}\right\} \quad \text{with} \quad (\mathbf{f}^-,\mathbf{m}^-) = (\mathbf{f}_1^-,\mathbf{m}_1^-) + (\mathbf{f}_{20}^-,\mathbf{m}_{20}^-) + (\mathbf{f}_{2D}^-,\mathbf{m}_{2D}^-) \tag{2}$$

in which $\overline{a}_0^k$ means to take the complex conjugate of a_0^k. This rule to denote the complex conjugate by the over line is applied to all first-order quantities in the following. The near-field formulation equivalent to that of Pinkster (1980) is written as :

$$\mathbf{f}_1^- = \frac{\rho g}{2}\oint_\Gamma d\ell\left[x_3^j\overline{\eta}^k + \overline{x}_3^k\eta^j - \eta^j\overline{\eta}^k\right]\mathbf{n} + \frac{\rho}{2}\iint_H ds\left[\nabla\phi^j\nabla\overline{\phi}^k + i\omega_k(\mathbf{x}^j\nabla\overline{\phi}^k + \mathbf{R}^j\wedge\overline{\phi}^k) - i\omega_j(\overline{\mathbf{x}}^k\nabla\phi^j + \overline{\mathbf{R}}^k\wedge\phi^j)\right]\mathbf{n} \tag{3a}$$

$$\mathbf{m}_1^- = \frac{\rho g}{2}\oint_\Gamma d\ell\left[x_3^j\overline{\eta}^k + \overline{x}_3^k\eta^j - \eta^j\overline{\eta}^k\right](\mathbf{r}\wedge\mathbf{n}) + \frac{\rho}{2}\iint_H ds\left[i\omega_k\overline{\phi}^k\mathbf{T}^j\wedge\mathbf{n} - i\omega_j\phi^j\overline{\mathbf{T}}^k\wedge\mathbf{n}\right]$$
$$+ \frac{\rho}{2}\iint_H ds\left[\nabla\phi^j\nabla\overline{\phi}^k + i\omega_k(\mathbf{x}^j\nabla\overline{\phi}^k + \mathbf{R}^j\wedge\overline{\phi}^k) - i\omega_j(\overline{\mathbf{x}}^k\nabla\phi^j + \overline{\mathbf{R}}^k\wedge\phi^j)\right](\mathbf{r}\wedge\mathbf{n}) \tag{3b}$$

for the first part. The second part includes the contribution of the second-order incoming waves :

$$(\mathbf{f}_{20}^-,\mathbf{m}_{20}^-) = -i(\omega_j-\omega_k)\rho\iint_H ds\,\phi_0^-(\mathbf{n},\mathbf{r}\wedge\mathbf{n}) \quad \text{with} \quad \phi_0^- = iA^-\frac{g^2\cosh k^-(z+h)/\cosh k^-h}{gk^-\tanh k^-h - (\omega_j-\omega_k)^2}e^{ik^-(x\cos\beta+y\sin\beta)} \tag{4}$$

in which $k^- = k_0^j - k_0^k$ and

$$A^- = \frac{\omega_j-\omega_k}{\omega_j\omega_k}k_0^jk_0^k\left[1+\tanh k_0^jh\tanh k_0^kh\right] + \frac{1}{2}\left[\frac{(k_0^j)^2/\omega_j}{\cosh^2 k_0^jh} - \frac{(k_0^k)^2/\omega_k}{\cosh^2 k_0^kh}\right]$$

and the contribution by the second-order diffraction potential which can be evaluated by Molin's method (1979) :

$$(\mathbf{f}_{2D}^-,\mathbf{m}_{2D}^-)_j = i(\omega_j-\omega_k)\rho\iint_H ds\left[\frac{\partial\phi_0^-}{\partial n} - \mathcal{N}_H^-\right]\psi_j^- + i(\omega_j-\omega_k)\frac{\rho}{g}\iint_F ds\,\mathcal{N}_F^-\psi_j^- \tag{5}$$

where ψ_j^- is the additional radiation potential at $(\omega_j-\omega_k)$. The terms $(\mathcal{N}_F^-,\mathcal{N}_H^-)$ are given by :

$$\mathcal{N}_F^- = i(\omega_j-\omega_k)\left[\nabla\phi^j\nabla\overline{\phi}_P^k + \nabla\phi_P^j\nabla\overline{\phi}_0^k\right] - \frac{i\omega_j}{2g}\left[\phi^j(-\omega_k^2\partial_z + g\partial_{zz}^2)\overline{\phi}_P^k + g(k_0^k)^2(1-\tanh^2 k_0^kh)\phi_P^j\overline{\phi}_0^k\right]$$
$$+ \frac{i\omega_k}{2g}\left[\overline{\phi}^k(-\omega_j^2\partial_z + g\partial_{zz}^2)\phi_P^j + g(k_0^j)^2(1-\tanh^2 k_0^jh)\overline{\phi}_P^k\phi_0^j\right] \tag{6a}$$

$$2\mathcal{N}_H^- = (i\omega_k\overline{\mathbf{x}}^k - \nabla\overline{\phi}^k)(\mathbf{R}^j\wedge\mathbf{n}) - (i\omega_j\mathbf{x}^j + \nabla\phi^j)(\overline{\mathbf{R}}^k\wedge\mathbf{n}) - (\mathbf{x}^j\nabla)\nabla\overline{\phi}^k\mathbf{n} - (\overline{\mathbf{x}}^k\nabla)\nabla\phi^j\mathbf{n} \tag{6b}$$

in which $\phi_P = \phi - \phi_0$ stands for the sum of the diffraction and radiation potentials.

In summary, the second-order low-frequency wave load is composed of one part (3) depending on the first-order quantities and another part on the second-order potential. The second part can be further decomposed into one resultant from the integration of incoming wave pressure (4), and another (5) composed of one integral on the hull and one integral over the free surface to represent the integration of diffraction wave pressure. The analysis in Chen (1994) shows that the free-surface integral is of order $O[(\omega_j - \omega_k)^2]$ or higher so that it can be ignored if the approximation of order $(\omega_j - \omega_k)$ is adopted and considered to be sufficient for most applications. Furthermore, the approximation by Pinkster (1980) showed that the hull integral in (5) involving the forcing term $\mathcal{N}_H$ can be neglected as well. In this way, the second part of low-frequency wave load is reduced to the sum of the incoming wave contribution (4) and the hull integral in (5) involving the normal gradient of incoming wave potential and the additional radiation potentials. Since the second-order potential of incoming waves (4) is analytical and the radiation potentials ψ_j^- can be evaluated with good precision, no numerical difficulty is present in the computation of this part of low-frequency loads. In the following, we are then concentrated on the accurate computation of the first part of low-frequency loads by using the middle-field formulation.

Middle-field formulation

In the particular case of $\omega_k = \omega_j$, the low-frequency wave load becomes constant drift load which is contributed only by the first part. The formulation (3) is called as the near-field one as it needs the evaluation of first-order wave field around the hull and along the waterline, as well as the first-order motions. Another formulation base on the momentum theorem for the horizontal drift forces has been developed by Maruo (1960) and extended to the moment around the vertical axis by Newman (1967). This formulation involving first-order wave field in the far field is often called far-field formulation and preferable in practice thanks to its better convergence and accuracy. Following the same procedure using the momentum theorem, Ferreira & Lee (1994) developed a middle-field formulation to evaluate the constant drift load.

Unlike the previous approach based on the momentum theorem for the drift load, the middle-field formulation for low-frequency load has been developed by Chen (2004). Starting with the near-field formulation and making use of the variants of Stokes' theorem given in Dai (1998), we obtain a new near-field formulation :

$$\mathbf{F}_1 = -\frac{\rho g}{2}\oint_\Gamma d\ell \left[\mathcal{E}^2\mathbf{n} - 2\mathcal{E}(\mathbf{Xn})\mathbf{k}\right] + \frac{\rho}{2}\iint_H ds \left[(\nabla\Phi\nabla\Phi)\mathbf{n} + 2\nabla\Phi_t(\mathbf{Xn})\right] \tag{7a}$$

$$\mathbf{M}_1 = -\frac{\rho g}{2}\oint_\Gamma d\ell \left[\mathcal{E}^2(\mathbf{r}\wedge\mathbf{n}) - 2\mathcal{E}(\mathbf{Xn})(\mathbf{r}\wedge\mathbf{k})\right] + \frac{\rho}{2}\iint_H ds \left[(\nabla\Phi\nabla\Phi)(\mathbf{r}\wedge\mathbf{n}) + 2(\mathbf{r}\wedge\nabla\Phi_t)(\mathbf{Xn})\right] \tag{7b}$$

which is essentially similar to (3) with some interesting improvements such as all terms with body motion $(\mathbf{T}, \mathbf{R})$ disappear and the term involving the displacement in the waterline integral gives a contribution only to the vertical components. Applying the Green theorem in a domain D surrounded by $S = H \cup C \cup F$ with the body hull H at its mean position, a fictitious (control) surface C surrounding the body and the mean free surface F limited by the intersection Γ of H with $z=0$ and that Γ_c of C with $z=0$, we obtain :

$$\mathbf{F}_1 = \rho g\oint_\Gamma d\ell\,\mathcal{E}(\mathbf{Xn})\mathbf{k} + \rho\iint_H ds\left[\nabla\Phi(\mathbf{X}_t\mathbf{n}) + \nabla\Phi_t(\mathbf{Xn})\right] - \rho\iint_F ds\left[(\Phi_z\nabla\Phi + \mathcal{E}\nabla\Phi_t) - (\mathcal{E}\Phi_{zt} + \nabla\Phi\nabla\Phi/2)\mathbf{k}\right] + \frac{\rho g}{2}\oint_{\Gamma_c} d\ell\,\mathcal{E}^2\mathbf{n} + \frac{\rho}{2}\iint_C ds\left[2\Phi_n\nabla\Phi - (\nabla\Phi\nabla\Phi)\mathbf{n}\right] \tag{8a}$$

$$\mathbf{M}_1 = \rho g\oint_\Gamma d\ell\,\mathcal{E}(\mathbf{Xn})(\mathbf{r}\wedge\mathbf{k}) + \rho\iint_H ds\,\mathbf{r}\wedge\left[\nabla\Phi(\mathbf{X}_t\mathbf{n}) + \nabla\Phi_t(\mathbf{Xn})\right] - \rho\iint_F ds\left[\mathbf{r}\wedge(\Phi_z\nabla\Phi + \mathcal{E}\nabla\Phi_t) - (\mathcal{E}\Phi_{zt} + \nabla\Phi\nabla\Phi/2)(\mathbf{r}\wedge\mathbf{k})\right] + \frac{\rho g}{2}\oint_{\Gamma_c} d\ell\,\mathcal{E}^2(\mathbf{r}\wedge\mathbf{n}) + \frac{\rho}{2}\iint_C ds\left[\Phi_n(\mathbf{r}\wedge\nabla\Phi) - (\nabla\Phi\nabla\Phi)(\mathbf{r}\wedge\mathbf{n})\right] \tag{8b}$$

The new formulation (8) is absolutely general as it can apply to the high-frequency loads as well as the low-frequency loads, to horizontal load components as well as vertical load components. The control surface C can be at a finite distance from the body or one pushed to infinity. In the first case, C may be pushed back to H while in the second case, C may be composed of the surface of a vertical cylinder plus the seabed. Furthermore, in the case of multiple bodies, the control surface C can be one surrounding an individual body and (8) gives the wave loads applied on the surrounded body.

An interesting feature of (8) concerns the low-frequency wave load for which the formulation is simplified. It can be easily checked that the values of the hull integral and of the first term in the free-surface integral are of order $O(\omega_j - \omega_k)$. Furthermore, the waterline integral as well as the second term in the free-surface integral contribute only to the vertical loads including the vertical force F_{1z}^- and moments around the horizontal axis

(M_{1x}^-, M_{1y}^-). Thus, the horizontal components $(F_{1x}^-, F_{1y}^-, M_{1z}^-)$ of low-frequency loads can be expressed as :

$$F_{1x}^- = \frac{\rho\omega_j\omega_k}{2g}\oint_{\Gamma_c} d\ell\,\phi^j\overline{\phi}^k n_1 + \frac{\rho}{2}\iint_C ds\,\left[\phi_n^j\overline{\phi}_x^k + \overline{\phi}_n^k\phi_x^j - \nabla\phi^j\nabla\overline{\phi}^k n_1\right] + (\omega_j-\omega_k)\delta F_{1x}^- \tag{9a}$$

$$F_{1y}^- = \frac{\rho\omega_j\omega_k}{2g}\oint_{\Gamma_c} d\ell\,\phi^j\overline{\phi}^k n_2 + \frac{\rho}{2}\iint_C ds\,\left[\phi_n^j\overline{\phi}_y^k + \overline{\phi}_n^k\phi_y^j - \nabla\phi^j\nabla\overline{\phi}^k n_2\right] + (\omega_j-\omega_k)\delta F_{1y}^- \tag{9b}$$

$$M_{1z}^- = \frac{\rho\omega_j\omega_k}{2g}\oint_{\Gamma_c} d\ell\,\phi^j\overline{\phi}^k n_6 + \frac{\rho}{2}\iint_C ds\,\left[\phi_n^j(x\overline{\phi}_y^k - y\overline{\phi}_x^k) + \overline{\phi}_n^k(x\phi_y^j - y\phi_x^j) - \nabla\phi^j\nabla\overline{\phi}^k n_6\right] + (\omega_j-\omega_k)\delta M_{1z}^- \tag{9c}$$

with the additional terms $(\delta F_{1x}^-, \delta F_{1y}^-, \delta M_{1z}^-)$ given by :

$$\delta F_{1x}^- = \frac{\rho}{2}\iint_H ds\,\left[\phi_n^j\overline{\phi}_x^k/\omega_j - \overline{\phi}_n^k\phi_x^j/\omega_k\right] - \frac{\rho}{2g}\iint_F ds\,\left[\omega_j\phi^j\overline{\phi}_x^k - \omega_k\overline{\phi}^k\phi_x^j\right] \tag{10a}$$

$$\delta F_{1y}^- = \frac{\rho}{2}\iint_H ds\,\left[\phi_n^j\overline{\phi}_y^k/\omega_j - \overline{\phi}_n^k\phi_y^j/\omega_k\right] - \frac{\rho}{2g}\iint_F ds\,\left[\omega_j\phi^j\overline{\phi}_y^k - \omega_k\overline{\phi}^k\phi_y^j\right] \tag{10b}$$

$$\delta M_{1z}^- = \frac{\rho}{2}\iint_H ds\,\left[\phi_n^j(x\overline{\phi}_y^k - y\overline{\phi}_x^k)/\omega_j - \overline{\phi}_n^k(x\phi_y^j - y\phi_x^j)/\omega_k\right] - \frac{\rho}{2g}\iint_F ds\,\left[\omega_j\phi^j(x\overline{\phi}_y^k - y\overline{\phi}_x^k) - \omega_k\overline{\phi}^k(x\phi_y^j - y\phi_x^j)\right] \tag{10c}$$

The formulations (9-10) provide, for the first time, an original way to evaluate the horizontal components of low-frequency wave loads. The additional terms given by (10) are of order $(\omega_j - \omega_k)$. If the body's motion is small $(\mathbf{X} \approx 0)$ in waves of small period, the integral over hull surface is negligible since $\phi_n = \mathbf{X}_t\mathbf{n}$ on H. The integral over the part of free surface is ease and accurate since the velocity potentials are not evaluated at body's surface.

Discussions and conclusion

In regular waves, the formulation (9) reduces to the first two integrals on the control surface since $\omega_j = \omega_k$. The low-frequency loads by (9) becomes the drift loads. If the control surface C is put to infinity, the expression (9) is in agreement with those by Maruo (1960) and Newman (1967). On the surface C at infinity, asymptotic expressions of the first-order potential can be used to simplify further the formulation to the single integrals involving the Fourier polar variable. This shows formally that the usual near-field formulation and far-field formulation are indeed equivalent.

The near-field, middle-field and far-field formulations are first compared in the computation of second-order drift loads on a LNG terminal of size (Length×Width×Draught = 350m× 50m× 15m) moored in water of finite depth (h =75m). The meshes of the hull composed of 1490 panels, and the control surfaces $C \cup F$ including the part of free surface F are illustrated on the left part of Figure 1. Only the half of the hull $(y \le 0)$ and that of $C \cup F$ for $(y \ge 0)$ are presented in the figure. On the right part of Figure 1, the non-dimensional values of drift load $F_{dy}/(\rho g L/2)$ with L=350m in waves of heading β=195° are depicted against the wave frequency (ω). Three meshes composed of 1490, 3816 and 7824 panels on the hull surface are used. The results using the near-

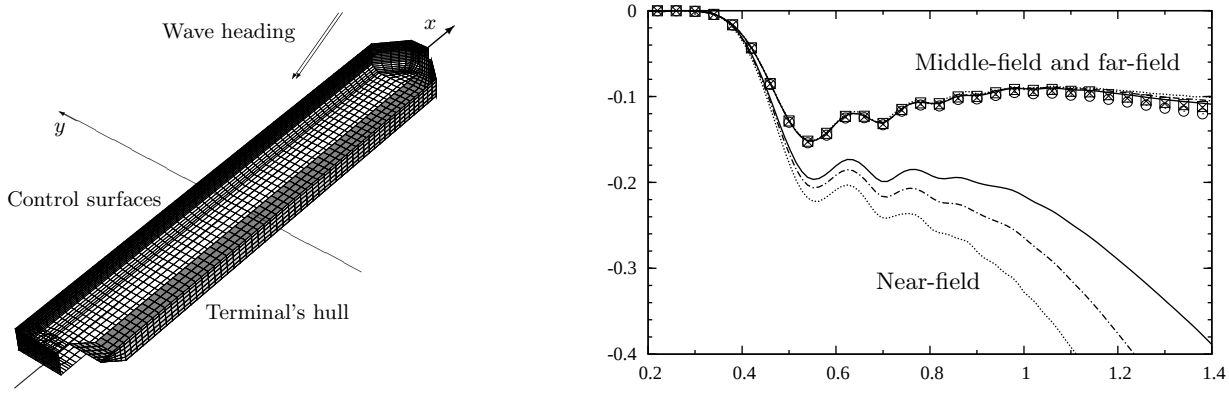

Figure 1: Mesh of terminal's hull & control surfaces (left) and drift loads $F_{dy}/(\rho g L/2)$ (right)

field and far-field formulations are represented by the dashed, dot-dashed and solid lines for three meshes (1490, 3616 and 7824 panels), respectively. The results using the middle-field formulation are shown by the symbols of circles (1490 panels), crosses (3616 panels) and squares (7924 panels). The curves associated with the near-field formulation are separated for $\omega > 0.45$ rad/s. This shows that the results using the near-field formulation are not convergent in most part of wave-frequency range. On the other side, the results obtained by the far-field

formulation (dashed, dot-dashed and solid lines) are indistinguishable on the whole range of wave frequency. The same feature is observed for the results associated with the middle-field formulation (circles, crosses and squares). Furthermore, the results of middle-field formulation are in excellent agreement with those of far-field formulation.

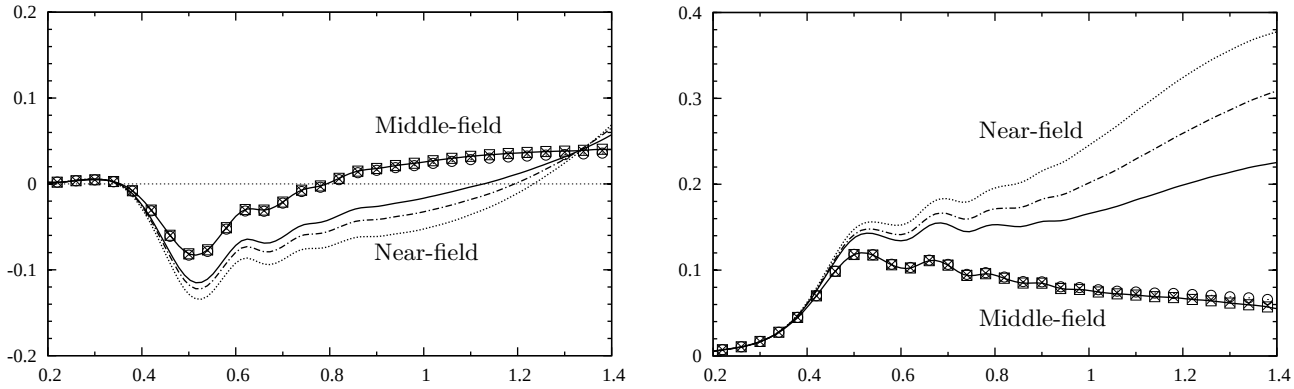

Figure 2: Real (left) and imaginary parts (right) $F_{1y}/(\rho g L/2)$ by using the near- and middle-field formulations

Now, we consider the low-frequency load $F_{1y}^{-}/(\rho g L/2)$ at a difference frequency $(\omega_j - \omega_k) = 0.04$ rad/s in waves of the same heading $\beta = 195°$. The results in complex are presented on Figure 2 against wave frequencies (ω_k). The real part and imaginary part of F_{1y} are depicted respectively on the left and right part of the figure. The results obtained by using the near-field formulation are illustrated by the dashed, dot-dashed and solid lines associated with the meshes of 1490, 3616 and 7924 panels, respectively. The results obtained from the middle-field formulation are shown by the symbols of circles, crosses and squares associated with three meshes. Again, we observe that the near-field formulation gives the results with poor precision while the middle-field formulation provides the results of excellent convergence.

The application of the middle-field formulation newly-obtained in Chen (2004) to the computation of second-order low-frequency loads confirms its important advantages. Firstly, it permits to make the connection between the near-field formulation derived from the pressure integration and the far-field formulation based on the momentum theorem for the constant drift load. Secondly, it accumulates the virtues of both near-field and far-field formulations, i.e. the excellent precision of far-field formulation and the access to the low-frequency wave loads as the near-field formulation. Furthermore, in the case of multiple bodies, the middle-field formulation provides the drift load as well as the low-frequency load on each individual body while the far-field formulation can only give the sum of drift loads on all bodies.

References

[1] Chen X.B. (1994) Approximation on the quadratic transfer function of low-frequency loads, *Proc. 7th Intl Conf. Behaviour Off. Structures*, BOSS'94, **2**, 289-302.

[2] Chen X.B. (2004) New formulations of the second-order wave loads. *Rapp. Technique, NT2840/DR/XC*, Bureau Veritas, Paris (France).

[3] Chen X.B. (2004) Hydrodynamics in offshore and naval applications - Part I. *Keynote lecture of 6th Intl. Conf. HydroDynamics*, Perth (Australia).

[4] Dai Y.S. (1998) Potential flow theory of ship motions in waves in frequency and time domain. (in Chinese). *The Express of the National Defense Industries*, Beijing (China).

[5] Ferreira M.D. & Lee C.H. (1994) Computation of second-order mean wave forces and moments in multibody interaction, *Proc. 7th Intl Conf. Behaviour Off. Structures*, BOSS'94, **2**, 303-13.

[6] Maruo H. (1960) The drift of a body floating on waves. *J. Ship Res.*,**4**, 1-10.

[7] Molin B. (1979) Second-order diffraction loads upon three-dimensional bodies. *App. Ocean Res.* **1**, 197-202.

[8] Newman J.N. (1967) The drift force and moment on ships in waves. *J. Ship Res.*, **11**, 51-60.

[9] Pinkster J.A. (1980) Low frequency second order wave exciting forces on floating structures. *H. Veenman En Zonen B.V. - Wageningen*, Wageningen (The Netherland).